Eur. Phys. J. C 46, 123–134 (2006)
Digital Object Identifier (DOI) 10.1140/epjc/s2005-02464-9

THE EUROPEAN PHYSICAL JOURNAL C

Unintegrated gluon distributions and Higgs boson production in proton–proton collisions

M. Łuszczak[2], A. Szczurek[1,2,a]

[1] Institute of Nuclear Physics PAN, 31-342 Cracow, Poland
[2] University of Rzeszów, 35-959 Rzeszów, Poland

Received: 12 September 2005 / Revised version: 20 October 2005 /
Published online: 9 February 2006 –

Abstract. Inclusive cross sections for Higgs boson production in proton–proton collisions are calculated in the formalism of unintegrated gluon distributions (UGDFs). Different UGDFs from the literature are used. Although they were constructed in order to describe the HERA deep-inelastic scattering F_2 data, they lead to surprisingly different results for Higgs boson production. We present both the two-dimensional invariant cross section as a function of Higgs boson rapidity and transverse momentum, as well as the corresponding projections on rapidity or transverse momentum. We quantify the differences between different UGDs by applying different cuts on interrelations between the transverse momentum of the Higgs and the transverse momenta of both fusing gluons. We focus on the large rapidity region. The interplay of the gluon–gluon fusion and weak-boson fusion in rapidity and transverse momentum is discussed. We find that above $p_{\rm t} \sim 50$–$100\,\mathrm{GeV}$ the weak-gauge boson fusion dominates over gluon–gluon fusion.

PACS. 12.38.Bx,12.38.Cy,13.85.Qk,14.70.Hp,14.80.Bn

1 Introduction

Recently unintegrated gluon (parton) distributions became a useful and intuitive phenomenological language for applications to many high-energy reactions (see e.g. [1,2] and references therein). Mostly the HERA F_2 data were used to test or tune different models of UGDFs. However, the structure function data are not the best tool to verify UGDF, in particular its dependence on gluon transverse momentum, because it enters in the $\gamma^* p$ total cross section in an integrated way. UGDFs have been used recently to describe jet correlations [3], correlations in heavy quark photoproduction [4], total cross section for Higgs production [5], inclusive spectra of pions in proton–proton collisions [6] or even nucleus–nucleus collisions [7]. It is rather obvious that differential cross sections seem a much better tool than the total or integrated cross sections to verify UGDFs.

Many unintegrated gluon distributions in the literature are ad hoc parametrizations of different sets of experimental data rather than derived from QCD. An example of a more systematic approach, making use of familiar collinear distributions can be found in [8]. Recently Kwieciński and collaborators [9–11] have shown how to solve the so-called CCFM equations by introducing unintegrated parton distributions in the space conjugated to the transverse momenta [9]. We present results for inclusive Higgs production based on unintegrated gluon distributions obtained by solving a set of coupled equations [11]. Recently these parton distributions were tested for inclusive gauge boson production in proton–antiproton collisions [12] and for charm–anticharm correlations in photoproduction [4].

While in the gauge boson production one tests mainly quark and antiquark (unintegrated) distributions at scales $\mu^2 \sim M_W^2, M_Z^2$, in the charm-quark photoproduction one tests mainly gluon distributions at scales $\mu^2 \sim m_c^2$. The non-perturbative aspect of UPDFs can be tested for soft pion production in proton–proton collisions [13].

Different ideas based on perturbative and non-perturbative QCD have been used in the literature to obtain the unintegrated gluon distributions in the small-x region. Since almost all of them were constructed to describe the HERA data it is necessary to test these distributions in other high-energy processes in order to verify the underlying concepts and/or approximations applied. It is the aim of this paper to show predictions of these quite different UGDFs for Higgs production at LHC at CERN although we are aware of the fact that a real test against future experimental data may be extremely difficult. We compare and analyze two-dimensional distributions for inclusive Higgs production in rapidity and transverse momentum $(y, p_{\rm t})$ to study the potential for such an analysis in the future. We focus not only on midrapidities but also try to understand the potential for studying UGDFs in more forward or backward rapidity regions. The results of the gluon–gluon fusion are compared with other mechanisms of Higgs boson production such as WW fusion for instance.

[a] e-mail: antoni.szczurek@ifj.edu.pl

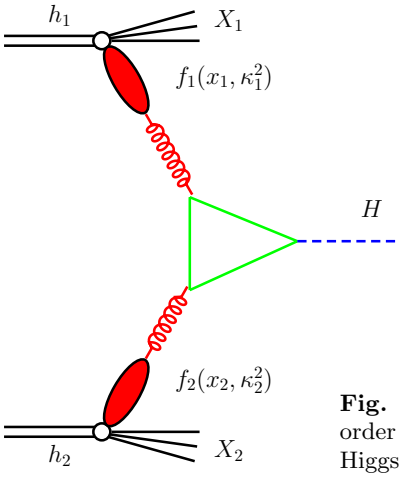

Fig. 1. Dominant leading-order diagram for inclusive Higgs production for $p_t \ll M_H$

2 Formalism

There are several mechanisms of the Higgs boson production which have been discussed in the literature. Provided that the Higgs mass is larger than 100 GeV and smaller than 600 GeV the gluon–gluon fusion (see Fig. 1) is the dominant mechanism of Higgs boson production at LHC energies [14]. The WW and ZZ fusion is the second important mechanism for the light-Higgs scenario. Often the so-called associated Higgs boson production (HW, HZ or $Ht\bar{t}$) is considered as a good candidate for the discovery of the Higgs boson. The contribution of the associated production to the inclusive cross section is, however, rather small. In the present paper we concentrate on the inclusive cross section and in particular on its dependence on rapidity and/or transverse momentum of the Higgs boson.

2.1 Gluon–gluon fusion

In the leading-order collinear factorization approach the Higgs boson has a zero transverse momentum. In the collinear approach the finite transverse momenta are generated only at next-to-leading order. However, the fixed-order approach is not useful for small transverse momenta and rather a resummation method must be used [16]. Recently Kwieciński, starting from the CCFM equation [15], has proposed a new method of resummation [17] based on unintegrated gluon distributions.

Limiting ourselves to small transverse momenta of the Higgs boson, i.e. small transverse momenta of the fusing gluons, the on-shell approximation for the matrix element seems a good approximation. There are also some technical reasons, to be discussed later, to stay with the on-shell approximation. In the on-shell approximation for the $gg \to H$ transition matrix element[1] the leading-order cross section in the unintegrated gluon distribution formalism reads[2]

$$\frac{\mathrm{d}\sigma^H}{\mathrm{d}y\mathrm{d}^2p_\mathrm{t}} = \sigma_0^{gg\to H} \int f_{g/1}\left(x_1,\kappa_1^2,\mu^2\right) f_{g/2}\left(x_2,\kappa_2^2,\mu^2\right) \times\delta^2\left(\boldsymbol{\kappa}_1+\boldsymbol{\kappa}_2-\boldsymbol{p}_\mathrm{t}\right)\frac{\mathrm{d}^2\kappa_1}{\pi}\frac{\mathrm{d}^2\kappa_2}{\pi}\,. \quad (1)$$

In the equation above the delta function assures conservation of transverse momenta in the gluon–gluon fusion subprocess. The $1/\pi$ factors are due to the definition of UGDFs. The momentum fractions should be calculated as $x_{1,2} = \frac{m_{t,H}}{\sqrt{s}}\exp(\pm y)$, where in comparison to the collinear case M_H is replaced by the Higgs transverse mass $m_{t,H}$. If we neglect transverse momenta and perform the following formal substitutions:

$$f_{g/1}\left(x_1,\kappa_1^2,\mu^2\right) \to x_1 g_1\left(x_1,\mu^2\right)\delta\left(\kappa_1^2\right)\,,$$
$$f_{g/2}\left(x_2,\kappa_2^2,\mu^2\right) \to x_2 g_2\left(x_2,\mu^2\right)\delta\left(\kappa_2^2\right)\,, \quad (2)$$

then we recover the well known leading-order formula

$$\frac{\mathrm{d}\sigma^H}{\mathrm{d}y\mathrm{d}^2p_\mathrm{t}} = \sigma_0^{gg\to H} x_1 g_1\left(x_1,\mu^2\right) x_2 g_2\left(x_2,\mu^2\right)\delta^2\left(\boldsymbol{p}_\mathrm{t}\right)\,. \quad (3)$$

The off-shell effects could be taken into account by inserting the $\gamma^*\gamma^* \to H$ off-shell cross section (corresponding to the matrix element squared $|\mathcal{M}^{gg\to H}(\boldsymbol{\kappa}_1,\boldsymbol{\kappa}_2)|^2$) under the integral in the formula (1) above. This will be discussed in more detail in a separate section.

There are a few conventions for UGDF in the literature. In the convention used throughout the present paper the unintegrated gluon distributions have dimension of GeV^{-2} and fulfill the approximate relation

$$\int_0^{\mu^2} f_\mathrm{g}\left(x,\kappa^2\left(,\mu^2\right)\right)\mathrm{d}\kappa^2 \approx x g_\mathrm{coll}\left(x,\mu^2\right)\,, \quad (4)$$

where $g_\mathrm{coll}(x,\mu^2)$ is the familiar conventional (integrated) gluon distribution. The scale μ^2 in the UGDF above is optional. In the effective Lagrangian approximation and assuming infinitely heavy top quark the cross section parameter $\sigma_0^{gg\to H}$ is given by [29]

$$\sigma_0^{gg\to H} = \frac{\sqrt{2}G_\mathrm{F}}{576\pi}\alpha_\mathrm{s}^2\left(\mu_r^2\right)\,. \quad (5)$$

In the following we shall take $\mu_r^2 = M_H^2$. Above we have assumed implicitly that the fusing gluons are on-mass-shell. In general, the fusing gluons are off-mass-shell. This effect was analyzed in detail in the production of Higgs associated with two jets [30]. The effect found there is small provided $M_H < 2m_\mathrm{t}$.

The UGDFs are the main ingredients in evaluating the inclusive cross section for Higgs production. Depending on the approach, some UGDFs [7, 24–26] in the literature depend on two variables, longitudinal momentum fraction x and transverse momentum κ^2; some in addition depend on a scale parameter [8–10, 27]. In the latter case the scale μ^2 is taken here as M_H^2 or ξM_H^2, where ξ is some factor.

[1] There is disagreement in the literature [19, 20] on how to include the off-shell effects.

[2] Some of the UGDFs from the literature depend only on the longitudinal momentum fraction and the transverse momentum of the virtual gluon. To keep the formulae below general we allow for a scale parameter needed in some distributions.

The seemingly 4-dimensional integrals in (1) can be written as 2-dimensional integrals after a suitable change of the variables $\boldsymbol{\kappa}_1, \boldsymbol{\kappa}_2 \to \boldsymbol{p}_\mathrm{t}, \boldsymbol{q}_\mathbf{t}$, where $\boldsymbol{p}_\mathrm{t} = \boldsymbol{\kappa}_1 + \boldsymbol{\kappa}_2$ and $\boldsymbol{q}_\mathrm{t} = \boldsymbol{\kappa}_1 - \boldsymbol{\kappa}_2$. Then

$$\frac{\mathrm{d}\sigma^H}{\mathrm{d}y\mathrm{d}^2p_\mathrm{t}} = \frac{\sigma_0^{gg\to H}}{(2\pi)^2} \int f_{g/1}\left(x_1, \kappa_1^2, \mu^2\right) f_{g/2}\left(x_2, \kappa_2^2, \mu^2\right) \mathrm{d}^2q_\mathrm{t}\,, \tag{6}$$

where $\boldsymbol{\kappa}_1 = \boldsymbol{p}_\mathrm{t}/2 + \boldsymbol{q}_\mathrm{t}/2$ and $\boldsymbol{\kappa}_2 = \boldsymbol{p}_\mathrm{t}/2 - \boldsymbol{q}_\mathrm{t}/2$. The integrand of this "reduced" 2-dimensional integral in $\boldsymbol{q}_\mathrm{t} = \boldsymbol{\kappa_1} - \boldsymbol{\kappa_2}$ is generally a smooth function of q_t and corresponding azimuthal angle ϕ_{q_t}.

2.1.1 Unintegrated gluon distributions

In the present analysis we shall use different unintegrated gluon distributions from the literature. We include gluon distributions corresponding to a simple saturation model used by Golec-Biernat and Wüsthoff to describe the HERA deep-inelastic data [24] (GBW), a saturation model of Kharzeev and Levin used to describe rapidity distributions of charged particles [7] (KL)[3], the Balitskij–Fadin–Kuraev–Lipatov (BFKL)-type UGDF [25] and three other distributions in the transverse-momentum space [8,27] (KMR) and [26] as well as the Kwieciński UGDF in the b-space. A more detailed description of almost all distributions mentioned above can be found e.g. in [6]. The Kwieciński UGDF as the only one defined in the b-space requires a separate discussion. It will be shown below that the formulae for the inclusive cross section for Higgs boson production via gluon–gluon fusion can be written in an equivalent way also in terms of distributions in the b-space.

2.1.2 Kwieciński gluon distribution and the inclusive cross section

Taking the following representation of the δ function:

$$\delta^2\left(\boldsymbol{\kappa_1} + \boldsymbol{\kappa_2} - \boldsymbol{p}_\mathrm{t}\right) = \frac{1}{(2\pi)^2} \int \mathrm{d}^2b \exp\left[(\boldsymbol{\kappa_1} + \boldsymbol{\kappa_2} - \boldsymbol{p}_\mathrm{t})\boldsymbol{b}\right], \tag{7}$$

(6) can be written in an equivalent way in terms of gluon distributions in the space conjugated to the gluon transverse momentum[4]

$$\frac{\mathrm{d}\sigma^H}{\mathrm{d}y\mathrm{d}^2p_\mathrm{t}} = \sigma_0^{gg\to H} \int \tilde{f}_{g/1}\left(x_1, b, \mu^2\right) \tilde{f}_{g/2}(x_2, b, \mu^2) J_0(p_\mathrm{t}b) 2\pi b \mathrm{d}b\,, \tag{8}$$

where

$$\tilde{f}_g\left(x, b, \mu^2\right) = \int_0^\infty \mathrm{d}\kappa_\mathrm{t}\kappa_\mathrm{t} J_0(\kappa_\mathrm{t}b) f_\mathrm{g}\left(x, \kappa_\mathrm{t}^2, \mu^2\right). \tag{9}$$

For most of the unintegrated gluon distributions (6) is used. Equation (8) is used when applying the Kwieciński unintegrated distributions obtained as a solution of his equations in the b-space. The b-space approach proposed by Kwieciński is very convenient to introduce the non-perturbative effects like intrinsic (non-perturbative) transverse-momentum distributions of partons in nucleons. It seems reasonable, at least in a first approximation, to include the non-perturbative effects in the factorizable way:

$$\tilde{f}_g\left(x, b, \mu^2\right) = \tilde{f}_g^{\mathrm{CCFM}}\left(x, b, \mu^2\right) \cdot F_g^{\mathrm{NP}}(b)\,. \tag{10}$$

The form factor responsible for the non-perturbative effects must be normalized such that

$$F_g^{\mathrm{NP}}(b = 0) = 1\,. \tag{11}$$

Then by construction

$$\tilde{f}_g\left(x, b = 0, \mu^2\right) = \frac{x}{2} g\left(x, \mu^2\right). \tag{12}$$

In the following, for simplicity, we use an x-independent form factor

$$F_g^{\mathrm{NP}}(b) = \exp\left(-\frac{b^2}{4b_0^2}\right), \tag{13}$$

which is responsible for the non-perturbative effects. The Gaussian form factor in b means also a Gaussian initial momentum distribution $\exp(-k_\mathrm{t}^2 b_0^2)$ (the Fourier transform of a Gaussian function is a Gaussian function). A Gaussian form factor is often used to correct collinear pQCD calculations for so-called intrinsic momenta. Other functional forms in b are also possible.

The similarities and differences between the standard soft gluon resummation and the CCFM resummation have been discussed recently in [17]. It has been shown how the soft gluon resummation formulae can be obtained as a result of the approximate treatment of the solution of the CCFM equation in the so-called b-representation.

2.1.3 Off-shell matrix element for $g^*g^* \to H$

While in the collinear approach the off-shell matrix elements are needed only at higher orders [19], in the k_t-factorization approach the off-shell matrix elements appear in principle already at the leading order. In [19] the matrix element was calculated in the framework of the effective Lagrangian for the Higgs boson coupling to gluons in the infinitely heavy top mass approximation. While the on-mass-shell couplings in the full theory and in the effective Lagrangian theory are equivalent, this is not expected for matrix element with off-shell gluons. In particular, the dependence on the transverse momenta and their relative orientation can be different. The use of the effective vertex all over the phase space may not be completely realistic.

[3] The normalization of the gluon distributions was fixed in [6] to reproduce the HERA data.

[4] The simple form of the formula below would not be possible with off-shell effects, i.e. when $|\mathcal{M}^{gg\to H}|^2$ is a function of $\boldsymbol{\kappa}_1$ and $\boldsymbol{\kappa}_2$.

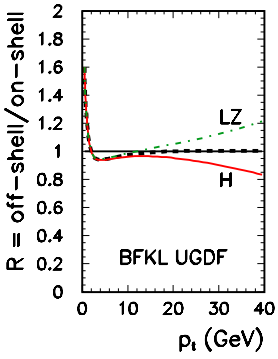

Fig. 2. The ratio R as a function of Higgs transverse momentum for the full range of Higgs rapidity. The thick dashed line corresponds to neglecting the function λ, i.e. assuming $\lambda = 1$. The solid line was obtained with the Hautmann prescription of the flux factor [19] while the dash-dotted line is based on the formula from [20]. In this calculation the BFKL UGDF was used as an example

However, the matrix element in the full theory (with finite top mass) has not yet been calculated.

In the present paper we shall only estimate the off-shell effects in the effective Lagrangian approximation. Then the cross section for the Higgs production can be written as

$$\frac{\mathrm{d}\sigma^H}{\mathrm{d}y\mathrm{d}^2p_\mathrm{t}} = \frac{\sigma_0^{gg\to H}}{(2\pi)^2}\int f_{g/1}\left(x_1,\kappa_1^2,\mu^2\right) f_{g/2}\left(x_2,\kappa_2^2,\mu^2\right) \times 2\frac{\left(\boldsymbol{\kappa}_1\cdot\boldsymbol{\kappa}_2\right)^2}{\kappa_1^2\kappa_2^2}\lambda\left(\kappa_1^2,\kappa_2^2,p_\mathrm{t}^2\right)\mathrm{d}^2q_\mathrm{t}\,, \tag{14}$$

where λ is a smooth function of its parameters [19, 20]. In the limit $p_\mathrm{t}^2 \to 0$, $\kappa_1^2 \to 0$, $\kappa_2^2 \to 0$ the dimensionless function $\lambda(\kappa_1^2,\kappa_2^2,p_\mathrm{t}^2) \to 1$. Then the $2\cos^2\phi_{\boldsymbol{\kappa}_1,\boldsymbol{\kappa}_2}$ factor in the formula above constitutes the essential difference with respect to the on-shell approximation. It modifies the dependence of the integrand under the ϕ_q integration.

In Fig. 2 we show the ratio

$$R = \frac{\left(\mathrm{d}\sigma/\mathrm{d}p_\mathrm{t}\right)_{\text{off-shell}}}{\left(\mathrm{d}\sigma/\mathrm{d}p_\mathrm{t}\right)_{\text{on-shell}}} \tag{15}$$

as a function of the Higgs-boson transverse momentum. In this calculation the BFKL unintegrated gluon distributions have been used as an example. The result for other distributions is similar. The final effect is rather small (less than 10%) in the region of our interest and depends on the way how the flux factor for off-shell gluons is defined [19, 20][5]. At finite, but not too large, Higgs boson transverse momenta the averaging over gluon transverse momenta with UGDFs gives $\langle 2\cos^2\phi_{\kappa_1,\kappa_2}\rangle \approx 1$, and one approximately recovers the on-shell result. This is not true for $p_\mathrm{t} \approx 0$, when $\boldsymbol{\kappa_1}$ and $\boldsymbol{\kappa_2}$ are strongly anticorrelated and the averaging is not efficient. The off-shell effect on the integrated cross section $(\mathrm{d}\sigma/\mathrm{d}y)$ is even smaller. Here we wish to concentrate rather on the effect of the transverse momenta inherent for UGDFs. We shall leave a detailed study of the off-shell effects in the effective Lagrangian and in the full theory for the future and consequently we shall use the on-shell matrix element in the following. This approximation will be also useful here when comparing the k_t-factorization results with that for the standard collinear and soft gluon resummation approaches. The on-shell approximation was used recently in the formalism od doubly unintegrated parton distribution for electroweak boson production [18].

[5] While it is rather straightforward to calculate the matrix element for off-shell gluons, there is some ambiguity in defining the flux factor for virtual gluons.

2.1.4 Standard soft gluon resummation

The formula for inclusive cross section in terms of unintegrated gluon distributions in the impact parameter space looks very similar to the one in the standard soft gluon resummation approach known from the literature. This similarity is not random [17]. In the Collins–Soper–Sterman (CSS) approach [16] the resummed cross section for Higgs production reads

$$\begin{aligned}\frac{\mathrm{d}\sigma}{\mathrm{d}y\mathrm{d}^2p_{\mathrm{t},H}} &= \frac{\sigma_0^{gg\to H}}{(2\pi)^2}\int \mathrm{d}^2b J_0(p_\mathrm{t}b) W_{gg}^{\mathrm{NP}}\left(b,x_1,x_2,\mu^2\right) \\ &\times x_1\cdot\left[g_1(x_1,\mu(b)) + \frac{\alpha_\mathrm{s}(\mu(b))}{2\pi}C_{vc}g_1(x_1,\mu(b)) + \frac{\alpha_\mathrm{s}(\mu(b))}{2\pi}\sum_{f_1}\left(C_{gq}\otimes q_1^{f_1}\right)(x_1,\mu(b))\right] \\ &\times x_2\cdot\left[g_2(x_2,\mu(b)) + \frac{\alpha_\mathrm{s}(\mu(b))}{2\pi}C_{vc}g_2(x_2,\mu(b)) + \frac{\alpha_\mathrm{s}(\mu(b))}{2\pi}\sum_{f_2}\left(C_{gq}\otimes q_2^{f_2}\right)(x_2,\mu(b))\right] \\ &\times \exp\left[\frac{1}{2}\left(S_g\left(b,\mu^2\right)+S_g\left(b,\mu^2\right)\right)\right]\,,\end{aligned} \tag{16}$$

where the exponents in the Sudakov-like form factors read

$$\begin{aligned}S_g\left(b,\mu^2\right) &= -\int_{\bar\mu^2_{\min}(b)}^{\mu^2}\frac{\mathrm{d}\bar\mu^2}{\bar\mu^2} \\ &\times\left[\ln\left(\frac{\mu^2}{\bar\mu^2}\right)A_g\left(\alpha_\mathrm{s}\left(\bar\mu^2\right)\right)+B_g\left(\alpha_\mathrm{s}\left(\bar\mu^2\right)\right)\right]\,.\end{aligned} \tag{17}$$

The coefficient functions C in (16) can be found in [21]. The coefficients A and B in the Sudakov-like form factor can be expanded in a series of α_s:

$$\begin{aligned}A_g &= 2C_A\frac{\alpha_\mathrm{s}(\bar\mu)}{2\pi}+\left(\frac{\alpha_\mathrm{s}(\bar\mu)}{2\pi}\right)^2(\ldots)+\ldots\,, \\ B_g &= -2\beta_0\frac{\alpha_\mathrm{s}(\bar\mu)}{2\pi}+\left(\frac{\alpha_\mathrm{s}(\bar\mu)}{2\pi}\right)^2(\ldots)+\ldots\,,\end{aligned} \tag{18}$$

where $\beta_0 = \frac{11}{6}C_A - \frac{2}{3}N_F T_R$ ($T_R = \frac{1}{2}$, $N_F = 5$, $C_A = 3$). The CSS formalism [16] leaves open the question of small b. Different prescriptions have been proposed to treat this

region. The lower limit of the integral in (17) is usually taken $\mu^2_{\rm min}(b) = \left(\frac{C_b}{b}\right)^2$, where $C_b = 2\exp(-\gamma_{\rm E}) \approx 1.1229$. This prescription leads to a kink for the Sudakov form factor if $C_b/b = \mu$. To allow for a smooth dependence and to guarantee that the lower limit is really lower than the upper limit, one could make the following replacement $\mu^2_{\rm min}(b) = \left(\frac{C_b}{b}\right)^2 \to \left(\frac{C_b}{b}\right)^2 \left[1 + C_b^2/(b^2\mu^2)\right]^{-1}$. To guarantee that the scale of parton distribution does not take an unphysically small value we shall use the following prescription:

$$\mu^2(b) = \mu^2_{\rm min}(b) + \mu_0^2 \,, \tag{19}$$

where μ_0^2 is the starting value for the QCD evolution. In the present paper we shall use easy to handle leading-order parton distributions from [28].

$W_{gg}^{\rm NP}(b, x_1, x_2, \mu^2)$ in (16) is of non-perturbative origin. Different effective parametrizations have been proposed in the literature. Assuming a factorizable form of the $W_{gg}^{\rm NP}$ function

$$W_{gg}^{\rm NP}\left(b, x_1, x_2, \mu^2\right) = F_g^{\rm NP}\left(b, x_1, \mu^2\right) \cdot F_g^{\rm NP}\left(b, x_2, \mu^2\right) \,, \tag{20}$$

the soft gluon resummation formula (16) and the unintegrated gluon distribution formula (8) for Higgs production in the b-space have an identical structure if the following formal assignment is made:

$$\tilde{f}_g^{\rm SGR}\left(x, b, \mu^2\right) = \frac{1}{2} F_g^{\rm NP}\left(b, x, \mu^2\right) \left[x g\left(x, \mu^2(b)\right) + \ldots\right] \times \exp\left(\frac{1}{2} S_g\left(b, \mu^2\right)\right) \,. \tag{21}$$

If the off-shell matrix element for $gg \to H$ is taken in the UGDF approach with the Kwieciński distribution, the structure of the formula in both approaches would be different. In this sense the UGDF approach seems more general than the b-space resummation method.

2.2 $2 \to 2$ processes

At sufficiently large transverse momenta ($p_{\rm t} > M_H$) the Higgs boson production of the type $2 \to 2$ should dominate over the $2 \to 1$ mechanism discussed above. The cross section for fixed-order processes of the type $p_1 p_2 \to H p_3$ (parton + parton $\to$ Higgs + parton) of the order of $\alpha_{\rm s}$ is well known [31]:

$$\frac{{\rm d}\sigma}{{\rm d}y_H {\rm d}y_p {\rm d}^2 p_{\rm t}}(y_W, y_p, p_{\rm t}) \tag{22}$$

$$= \frac{1}{16\pi^2 \hat{s}^2} \left\{ x_1 g_1\left(x_1, \mu^2\right) x_2 g_2\left(x_2, \mu^2\right) \overline{|\mathcal{M}_{gg\to Hg}|^2} \right.$$

$$+ \left[\sum_{f_1=-3,3} x_1 q_{1,f_1}\left(x_1, \mu^2\right)\right] x_2 g_2\left(x_2, \mu^2\right) \overline{|\mathcal{M}_{qg\to Hq}|^2}$$

$$+ x_1 g_1\left(x_1, \mu^2\right) \left[\sum_{f_2=-3,3} x_2 q_{2,f_2}\left(x_2, \mu^2\right)\right] \overline{|\mathcal{M}_{gq\to Hq}|^2}$$

$$\left. + \sum_{f=-3,3} x_1 q_{1,f}\left(x_1, \mu^2\right) x_2 q_{2,-f}\left(x_2, \mu^2\right) \overline{|\mathcal{M}_{qq\to Hg}|^2} \right\} .$$

The indices f in the formula above number both quarks ($f > 0$) and antiquarks ($f < 0$). Only three light flavors are included in the actual calculations. The explicit formulae for $\overline{|\mathcal{M}|^2}$ can be found in [31].

2.3 Weak-boson fusion

Up to now we have discussed only the contribution of the dominant LO gluon–gluon fusion and NLO $2 \to 2$ corrections and completely ignored contributions of other processes. The second most important mechanism for Higgs production is the fusion of off-shell gauge bosons: WW or ZZ. It is known that at LHC energy and intermediate mass ($100\,{\rm GeV} < M_H < 500\,{\rm GeV}$) Higgs the WW fusion constitutes about 10–15% of the integrated inclusive cross section. If the weak-boson fusion contribution was separated, the measurement of the WWH (or ZZH) coupling would be very interesting test of the standard model.

Previous studies of the WW mechanism concentrated on the total cross section for the Higgs production. In the present paper we are interested in differential distributions of the Higgs boson rather than in the integrated cross section.

For the gauge boson fusion the partonic subprocess is of the $2 \to 3$ type: $q(p_1) + q(p_2) \to q(p_3) + q(p_4) + H(p_H)$. The corresponding hadronic cross section can be written as

$$\begin{aligned} {\rm d}\sigma = {} & \mathcal{F}_{12}^{VV}\left(x_1, x_2\right) \frac{1}{2\hat{s}} \overline{|\mathcal{M}_{qq\to qqH}|^2} \\ & \times \frac{{\rm d}^3 p_3}{(2\pi)^3 2E_3} \frac{{\rm d}^3 p_4}{(2\pi)^3 2E_4} \frac{{\rm d}^3 p_H}{(2\pi)^3 2E_H} \\ & \times (2\pi)^4 \delta^4(p_1 + p_2 - p_3 - p_4 - p_H) {\rm d}x_1 {\rm d}x_2 \,. \end{aligned} \tag{23}$$

The next-to-leading order corrections to the matrix element of the WW fusion are rather small [32]. For comparison the NLO corrections for gluon–gluon fusion are significantly larger. Since we wish to concentrate on relative effects of the gluon–gluon and WW fusion contributions in the following we restrict ourselves to a much simpler leading-order (LO) calculation. The LO subprocess matrix element was calculated first in [33]. The spin averaged matrix element squared reads

$$\overline{|\mathcal{M}|^2} = 128\sqrt{2} G_{\rm F}^3 \frac{M_W^8 (p_1 \cdot p_2)(p_3 \cdot p_4)}{\left(2p_3 \cdot p_1 + M_W^2\right)^2 \left(2p_4 \cdot p_2 + M_W^2\right)^2} \,. \tag{24}$$

For the WW fusion, limiting ourselves to light flavors, the partonic function is

$$\begin{aligned} & \mathcal{F}_{12}^{WW}\left(x_1, x_2\right) \\ & = \left(u_1\left(x_1, \mu_1^2\right) + \bar{d}_1\left(x_1, \mu_1^2\right) + \bar{s}_1\left(x_1, \mu_1^2\right)\right) \\ & \quad \times \left(\bar{u}_2\left(x_2, \mu_2^2\right) + d_2\left(x_2, \mu_2^2\right) + s_2\left(x_2, \mu_2^2\right)\right) \end{aligned}$$

$$+\left(\bar{u}_1\left(x_1,\mu_1^2\right)+d_1\left(x_1,\mu_1^2\right)+s_1\left(x_1,\mu_1^2\right)\right) \quad (25)$$
$$\times\left(u_2\left(x_2,\mu_2^2\right)+\bar{d}_2\left(x_2,\mu_2^2\right)+\bar{s}_2\left(x_2,\mu_2^2\right)\right) .$$

We take either
(i) $\mu_1^2=\mu_2^2=M_H^2$ or
(ii) $\mu_1^2=-t_1, \mu_2^2=-t_2$, where t_1 and t_2 are the virtualities of the W bosons. It is convenient to introduce the following new variables:

$$\boldsymbol{p}_+=\boldsymbol{p}_3+\boldsymbol{p}_4\,,$$
$$\boldsymbol{p}_-=\boldsymbol{p}_3-\boldsymbol{p}_4\,, \quad (26)$$

which allow one to eliminate the momentum-dependent $\delta^3(\ldots)$ in (23). Instead of integrating over x_1 and x_2 we shall integrate over $y_1\equiv\ln(1/x_1)$ and $y_2\equiv\ln(1/x_2)$. Then using (23) we can write the inclusive spectrum of the Higgs as

$$\frac{\mathrm{d}\sigma}{\mathrm{d}y\mathrm{d}^2p_\mathrm{t}} \quad (27)$$
$$=\int \mathrm{d}y_1\mathrm{d}y_2x_1x_2\mathcal{F}\left(x_1,x_2,\mu_1^2,\mu_2^2\right)\frac{1}{2\hat{s}}\frac{\mathrm{d}^3p_-}{16}\overline{|\mathcal{M}_{qq\to qqH}|^2}$$
$$\times\frac{1}{2E_3}\frac{1}{2E_4}\frac{1}{(2\pi)^5}\delta(E_1+E_2-E_3-E_4-E_H)\,.$$

This is effectively a four-dimensional integral which can be easily calculated numerically.

3 Results

3.1 Gluon–gluon fusion

Since we wish to concentrate on the potential to verify different UGDFs rather than to present the best predictions for LHC experiments we shall consider only one mass of the Higgs boson, $M_H=125\,\mathrm{GeV}$, as an example. This is slightly above the lower limit obtained from the analysis of the LEP data [34]. In addition, this is a mass for which many calculations in the literature have been performed recently. Therefore this gives an opportunity for comparison to the existing results.

Before we go to the analysis of the two-dimensional spectra of the Higgs boson produced in proton–proton or proton–antiproton collisions let us show the range of the gluon longitudinal momentum fraction tested in these processes. In Fig. 3 we present respectively x_1 and x_2 as a function of Higgs boson rapidity for a few different values of Higgs transverse momentum. While at Tevatron energies (panel (a)) only intermediate and large xs come into the game, in collisions at LHC energy (panel (b)) $x\sim10^{-2}$ is sampled at midrapidity. However, at LHC energy, at rapidities $|y|>2$ one enters the region of $x>0.1$. Here some of the low-x models of UGDFs may become invalid.

Let us concentrate first on the transverse-momentum distributions. The distribution of the Higgs transverse momentum (rapidity integrated) is shown in Fig. 4. In Fig. 5 we present the transverse-momentum distribution of the Higgs boson in different bins of rapidity specified in the figure caption. At midrapidity (panel (a)) only small xs are sampled. Even here different models from the literature give quite different transverse-momentum distributions, although all of them give a reasonable description of the HERA data. The LO soft gluon resummation distribution and the distribution obtained with the Kwieciński unintegrated gluon distribution ($b_0=1\,\mathrm{GeV}^{-1}$) are very similar with maxima at $p_{\mathrm{t},H}\approx10\,\mathrm{GeV}$ and $p_{\mathrm{t},H}\approx5\,\mathrm{GeV}$, respectively. The cross section for W or Z production is fairly sensitive to the choice of the non-perturbative form factor [12]. In contrast to the gauge boson production the

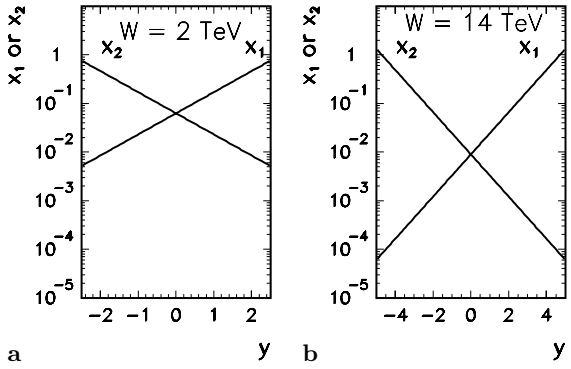

Fig. 3. x_1 and x_2 as a function of Higgs rapidity y for $p_\mathrm{t}=0$. In panel **a** for Tevatron energy $\sqrt{s}=2\,\mathrm{TeV}$ and in panel **b** for LHC energy $\sqrt{s}=14\,\mathrm{TeV}$

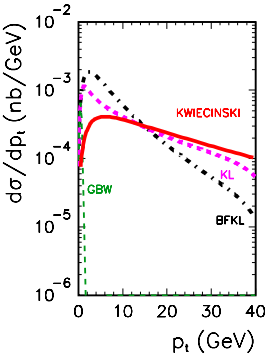

Fig. 4. Transverse momentum distribution of Higgs boson at LHC energy $W=14\,\mathrm{TeV}$ for different UGDFs from the literature: solid lines for the Kwieciński, thick dashed lines for the KL, thin dashed lines for the GBW, and the dash-dotted lines for the BFKL one

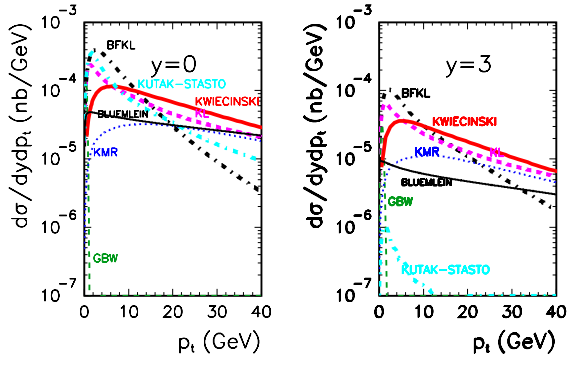

Fig. 5. Transverse momentum distribution of Higgs boson at LHC energy $W=14\,\mathrm{TeV}$ and y = 0 (left panel) and $y=\pm3$ (right panel) for different UGDFs from the literature. The notation here is the same as in the previous figure. In addition to the previous figure we present results for the KMR (dotted), the Kutak–Staśto (grey dash-dotted) and the Bluemlein (thin solid) UGDF

Higgs boson production is much less sensitive to the parameter of the Gaussian form factor. The results with $b_0 = 0.5$ or $2\,\mathrm{GeV}^{-1}$ (not shown here) almost coincide with the result for $b_0 = 1\,\mathrm{GeV}^{-1}$. Therefore in the following in all calculations we shall use $b_0 = 1\,\mathrm{GeV}^{-1}$. The BFKL-type gluon distributions lead to a much larger cross section at small Higgs transverse momenta and a sizeably larger slope of the p_t-distribution. The rapid fall-off of the cross section for the Golec-Biernat–Wüsthoff non-perturbative gluon distribution [24] (thin dashed curve) demonstrates how important the perturbative initial state radiation is in generating larger transverse momenta of the Higgs boson. Such effects are not taken into account in [24].

A comment regarding the GBW distribution is here in order. This distribution was obtained based on a simple dipole parametrization of the HERA data inspired by the saturation idea. In addition to the very steep distribution in the Higgs-boson transverse momentum the scale-independent GBW gluon distribution gives a very small total cross section (about half of 1 pb). One has to remember, however, that this distribution was constructed in order to describe $\sigma^{\mathrm{tot}}_{\gamma^* p}(Q^2)$ for small photon virtualities. We wish to stress here that this distribution is not an universal object. For example in its simplest form it fails to describe $\sigma^{\mathrm{tot}}_{\gamma^* p}(Q^2)$ for large photon virtualities. The corresponding effective gluon distribution defined as

$$x g_{\mathrm{GBW}}(x) \equiv \int_0^\infty \mathcal{F}_g^{\mathrm{GBW}}(x) \mathrm{d}\kappa^2 \tag{28}$$

resembles the standard collinear distribution $x g_{\mathrm{DGLAP}}(x, \mu^2)$ for small factorization scale $\mu^2 \sim 1\,\mathrm{GeV}^2$. The latter, when substituted into the standard leading-order formula, also leads to a small total cross section of the order of 1 pb. A reasonable total cross section is obtained provided $\mu^2 \sim M_H^2$. Although $g_{\mathrm{DGLAP}}(x, \mu^2 = 1\,\mathrm{GeV}^2)$ leads to a reasonable description of F_2 at $Q^2 \sim 1\,\mathrm{GeV}^2$, it cannot be directly (without DGLAP evolution) used for Higgs production. In this context the scale-independent GBW distribution should be understood as an initial condition for QCD evolution rather than an universal object to be used in different high-energy processes.

Different UGDFs constructed in order to describe the total cross section for the $\gamma^* p$ process give quite different predictions for the Higgs production. This, as will be discussed below, is not completely surprising. While the $\gamma^* p$ total cross section is sensitive to the integral $\int \mathrm{d}k_\mathrm{t}^2 f_g(x, k_\mathrm{t}^2(, \mu^2))$, the Higgs boson transverse-momentum distribution samples details of the unintegrated gluon distributions. As discussed in the previous section, in the case of Higgs boson production the inclusive cross section is a convolution of two UGDFs. In general, exclusive reactions are a much better place for testing UGDFs. In this sense the standard procedure to constrain UGDFs through describing the F_2 HERA data does not seem very effective.

In order to understand the situation somewhat better in Fig. 6 we show the corresponding average values of sampled transverse momenta as a function of Higgs transverse momentum. At $y = 0$, by symmetry requirement, $\langle \kappa_1 \rangle$ and $\langle \kappa_2 \rangle$ are identical. It is not the case for

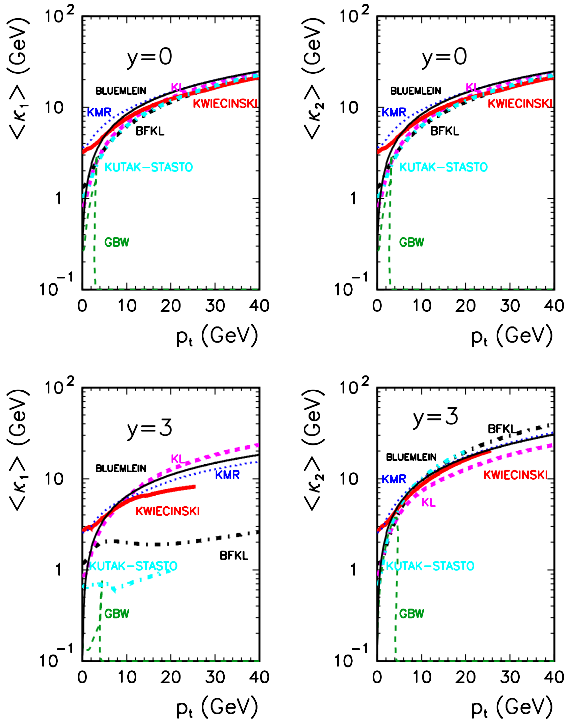

Fig. 6. Average gluon transverse momentum as a function of Higgs transverse momentum at LHC energy $W = 14\,\mathrm{TeV}$ for different UGDFs from the literature

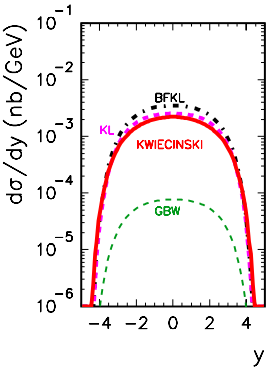

Fig. 7. Rapidity distribution of Higgs at LHC energy $W = 14\,\mathrm{TeV}$ for different UGDFs from the literature

$y = 3$. Rather similar results are obtained with different UGDFs. At very small Higgs transverse momenta one tests $\kappa \sim 1\,\mathrm{GeV}$. At large Higgs transverse momenta and $y = 0$ we get $\langle \kappa_1 \rangle + \langle \kappa_2 \rangle \approx p_\mathrm{t}/2$. Of course by symmetry $\langle \kappa_{1/2} \rangle(-y) = \langle \kappa_{2/1} \rangle(y)$.

Some examples of inclusive rapidity distributions are shown in Fig. 7. Even here the differences between different UGDFs are clearly visible. Above $|y| > 3$ only the resummation distribution (thin solid line), the Kwieciński distribution (thick solid line) and the Kimber–Martin–Ryskin one (dotted line) are applicable by construction. The other distributions were obtained by extending the generally small-x gluon distributions above $x > 0.1$ by multiplying the original formulae by $(1 - x)^n$. The power $n = 5$–7 was found recently in the production of $c\bar{c}$ pairs in photon–proton scattering at low energies [4]. In the present paper we used $n = 7$. Small differences may be expected only at the very

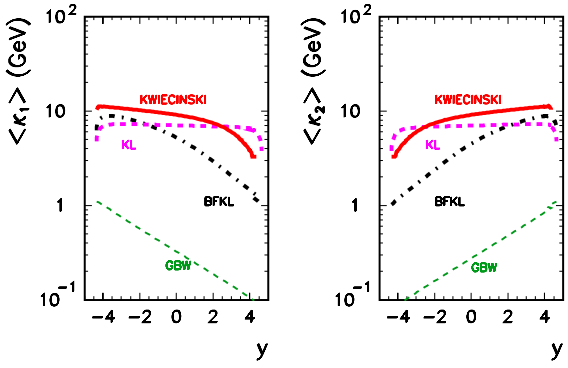

Fig. 8. Average gluon transverse momentum $\langle\kappa_1\rangle$ or $\langle\kappa_2\rangle$ as a function of Higgs rapidity for different UGDFs from the literature. In this calculation $p_t < 40\,\mathrm{GeV}$

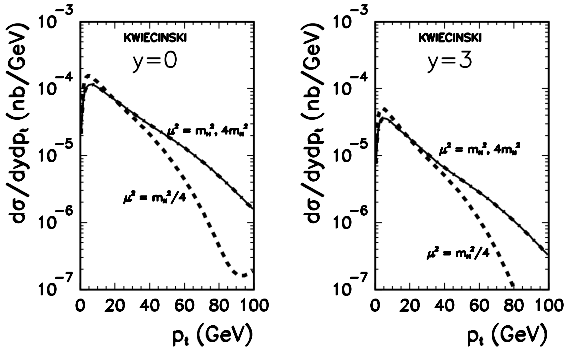

Fig. 9. Dependence of the result on the choice of the factorization scale for the Kwieciński UGDF for $y = 0$ (left panel) and $y = 3$ (right panel). In this calculation a Gaussian form factor with $b_0 = 1\,\mathrm{GeV}^{-1}$ was used

edges of the phase space, i.e. in the region we are not interested in here.

For completeness in Fig. 8 we show the average values of the gluon transverse momenta $\langle\kappa_1\rangle$ and $\langle\kappa_2\rangle$ as a function of the Higgs-boson rapidity. At midrapidity by symmetry $\langle\kappa_1\rangle \approx \langle\kappa_2\rangle$. The average values strongly depend on the UGDF used and on the region of rapidity. The asymmetry of the average values of the transverse momenta at forward/backward regions are closely related to Fig. 3 due to correlation of the transverse momenta with longitudinal momentum fractions. Generally, the smaller x_1 (x_2) the larger $\langle\kappa_1\rangle$ ($\langle\kappa_2\rangle$). The details depend, however, on the specific version of the gluon dynamics. The extremely small average transverse momenta for the GBW UGDF can be understood in the light of the discussion above.

How important is the choice of the factorization scale in our calculations with the Kwieciński UGDF? In Fig. 9 we show results obtained with quite different choices of factorization scale and with $b_0 = 1\,\mathrm{GeV}^{-1}$. There is very little effect if the factorization scale is increased from our cannonical value $\mu^2 = M_H^2$. There is, however, a sizeable effect if the factorization scale is decreased drastically, especially at $p_t > 50\,\mathrm{GeV}$. The factorization scale dependence in our case seems somewhat weaker than in a recent work [20].

It is particularly interesting to compare the results obtained with the Kwieciński unintegrated gluon distribu-

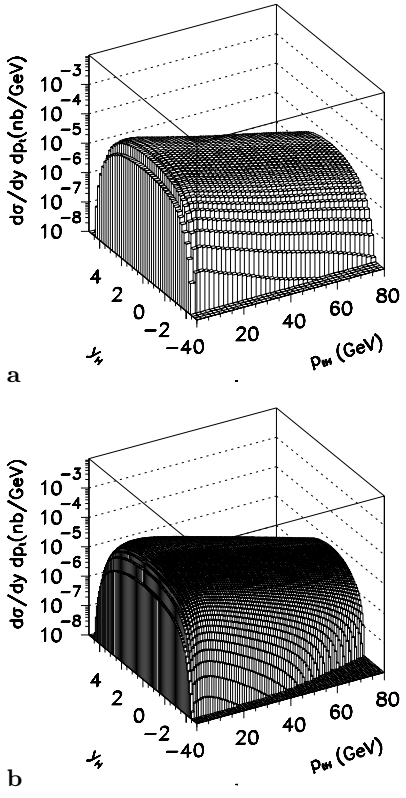

Fig. 10. A comparison of two-dimensional distributions of the Higgs boson for **a** the Kwieciński UGDF, **b** the LO b-space resummation

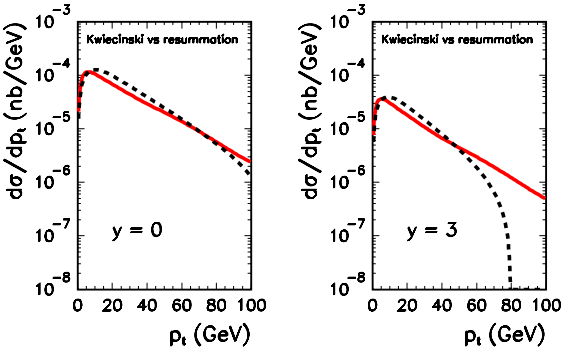

Fig. 11. A comparison of the Higgs transverse-momentum distribution calculated with the Kwieciński UGDF (red, solid) and the LO b-space resummation (black, dashed) for different rapidities: $y = 0$ (left panel) and $y = 3$ (right panel)

tions with those obtained from the standard soft gluon resummation method. In Fig. 10 we show two-dimensional distributions in (y, p_t). The distribution obtained with the Kwieciński UGDF decrease less rapidly with the Higgs transverse momentum than the distribution obtained in the standard soft gluon resummation. This is partially due to the different choice of the factorization scale in both methods.

A more detailed comparison is made in Fig. 11 where we have selected two rapidities $y = 0$ and $y = 3$. While at $y = 0$ the result obtained with Kwieciński distributions and that obtained within the standard resummation

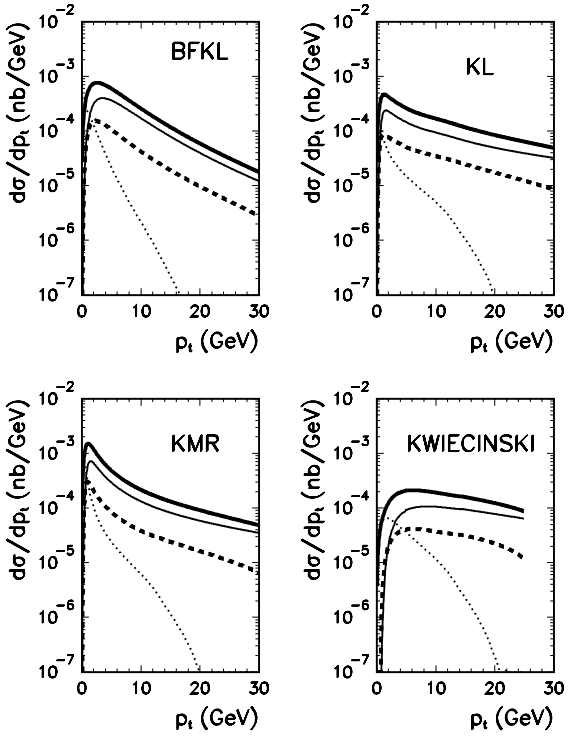

Fig. 12. Decomposition of the transverse-momentum distribution of Higgs boson at LHC energy $W = 14\,\mathrm{TeV}$ and $-1 < y < 1$ into four regions specified in the text. The thick solid line is a sum of all 4 contributions: thin solid lines for region I, dashed lines for region II + III, and dotted lines for region IV

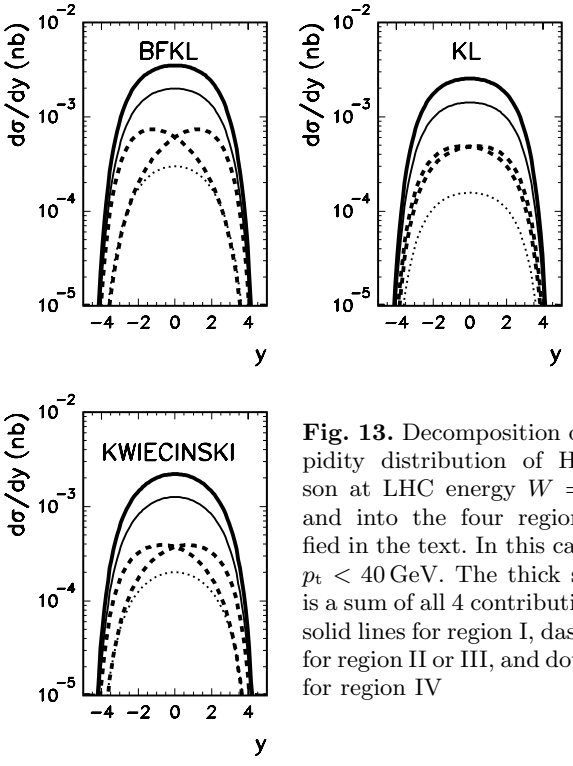

Fig. 13. Decomposition of the rapidity distribution of Higgs boson at LHC energy $W = 14\,\mathrm{TeV}$ and into the four regions specified in the text. In this calculation $p_\mathrm{t} < 40\,\mathrm{GeV}$. The thick solid line is a sum of all 4 contributions: thin solid lines for region I, dashed lines for region II or III, and dotted lines for region IV

method almost coincide, they become quite different at $y = 3$ and $p_\mathrm{t} > 60\,\mathrm{GeV}$. However, the applicability of both methods at large transverse momenta is not obvious. The result for $y = 3$ at large transverse momenta obtained with the Kwieciński UGDF seems more trustworthy than that obtained within the standard resummation method. The problems of the standard resummation method at large transverse momenta may be caused by some somewhat arbitrary prescriptions used as discussed in Sect. 2.

In order to better emphasize the differences between different UGDFs we separate the contributions to the integral in (6) from four different disjoint and complementary kinematic regions:
(I) $\kappa_1 < p_\mathrm{t}$ and $\kappa_2 < p_\mathrm{t}$,
(II) $\kappa_1 < p_\mathrm{t}$ and $\kappa_2 > p_\mathrm{t}$,
(III) $\kappa_1 > p_\mathrm{t}$ and $\kappa_2 < p_\mathrm{t}$,
(IV) $\kappa_1 > p_\mathrm{t}$ and $\kappa_2 > p_\mathrm{t}$, where κ_1 and κ_2 are the transverse momenta of the last gluons in the ladders and p_t is the transverse momentum of the produced Higgs boson. In Fig. 12 we present the decomposition of the Higgs cross section $\frac{\mathrm{d}\sigma}{\mathrm{d}p_\mathrm{t}}$ into those four regions as a function of the Higgs transverse momentum. Here we limit ourselves to midrapidities ($-1 < y < 1$) only. In the case of the Kwieciński UGDF, first the Fourier transform from the b-space to the κ_t-space was calculated and the results were stored on the grid in x and κ_t^2. The grid was used then for interpolation when using formula (6) with the extra conditions on the transverse momenta specified above. It is interesting to note that at larger transverse momenta the contributions from regions II, III and IV are completely negligible. The other contributions are important only at very low transverse momenta. For completeness in Fig. 13 we show a similar decomposition as a function of rapidity. In this calculation we have limited Higgs transverse momenta to $p_\mathrm{t} < 40\,\mathrm{GeV}$. The contribution of region I dominates at midrapidities. The contribution of the asymmetric (in κ_1 and κ_2) regions II and III becomes important at very forward or very backward Higgs production. The contribution of region IV is negligible almost everywhere. The proportions of contributions corresponding to the four specified above regions differ significantly for different UGDFs.

3.2 Estimates of higher-order effects

In the present paper we have limited ourselves to the leading-order approach only. This was dictated by the fact that until now only a leading-order approach was used to describe the HERA data in terms of UGDFs. Furthermore the consistent next-to-leading order analysis is rather complicated. We leave the next-to-leading order analysis for a future study. Instead, we wish to visualize (estimate) the NLO corrections in a similar soft gluon resummation approach where the relevant formalism was worked out in detail [21]. In Fig. 14 we present the relevant soft gluon resummation K-factor as a function of Higgs transverse momentum for $-0.5 < y < 0.5$ (panel a) and $2.5 < y < 3.5$ (panel b). In this calculation the Gaussian form factor (see (13)) with $b_0 = 1\,\mathrm{GeV}^{-1}$ was used. The dashed line includes only gluonic NLO corrections to the partonic function, the dotted line exclusively the quark NLO corrections and the

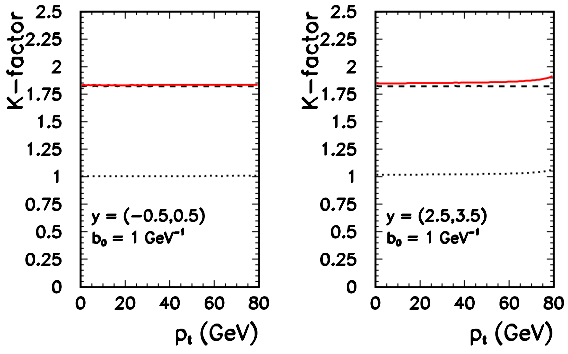

Fig. 14. NLO K-factor in the soft gluon resummation formalism as a function of the Higgs transverse momentum for two different bins of rapidity. The dashed line corresponds to separated gluonic contributions, and the dotted line to separated quarkish contributions. The solid line is for both effects included simultaneously

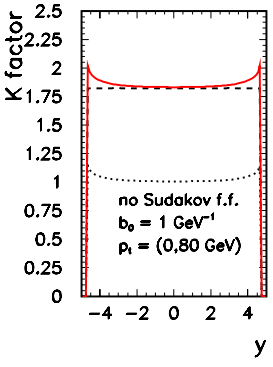

Fig. 15. NLO K-factor in the soft gluon resummation formalism as a function of Higgs rapidity. In this calculation $p_t < 80\,\mathrm{GeV}$. The meaning of the curves here is the same as in the previous figure

solid line includes all NLO effects altogether. At midrapidities the gluonic effects are absolutely dominant and enhance the leading-order cross section by about 80%. The quark corrections are at the level of 1% and can be numerically neglected. They become sizeable (of the order of 10%) at very forward and very backward rapidities. In Fig. 15 we present a corresponding K-factor ($K = \mathrm{NLO/LO}$) as a function of the Higgs rapidity. In this calculations $p_{t,H} < 80\,\mathrm{GeV}$ was assumed. Summarizing, to a good approximation the NLO soft gluon resummation corrections result in multiplying the LO cross section for Higgs production by a factor of about 1.8.

Up to now we have concentrated on relatively small Higgs transverse momenta. At high transverse momenta the standard $2 \to 2$ mechanisms take over. The cross section for perturbative $2 \to 2$ processes with Higgs in the final state is shown in Fig. 16. The $gg \to Hg$ dominates at small transverse momenta and midrapidities. The $qg \to Hq$ and $gq \to Hq$ become comparable to the first contribution at large transverse momenta and forward and backward regions, respectively. The contribution of $qq \to Hg$ is negligible all over the interesting part of the phase space.

3.3 Weak boson fusion versus gluon–gluon fusion

The weak-boson fusion is known to be another important ingredient in the total (integrated) cross section for Higgs boson production [14]. It is interesting to ask: what is the interrelation between the two dominant contributions in rapidity and transverse momentum of the Higgs boson? In Fig. 17 we present such a two-dimensional spectrum. This spectrum is very different from those for the gluon–gluon

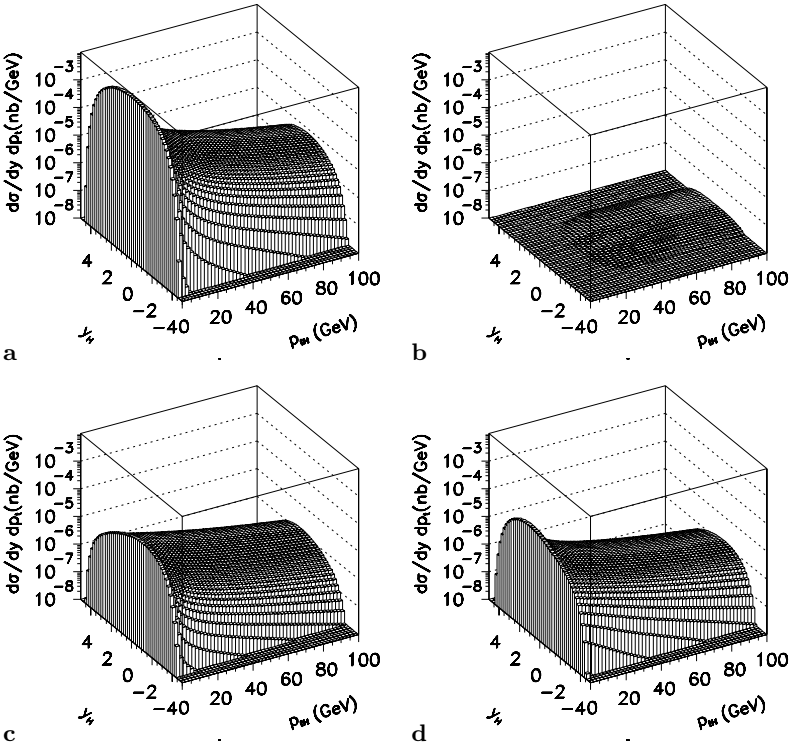

Fig. 16. Contributions of different subprocesses of the $2 \to 2$ type for $W = 14\,\mathrm{TeV}$, respectively for **a** gg, **b** qq, **c** qg and **d** gq

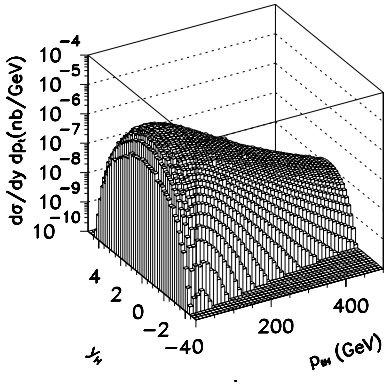

Fig. 17. Two-dimensional distribution in y and p_t of Higgs from the LO WW fusion process. In this calculation we have taken $\mu_1^2 = \mu_2^2 = M_H^2$

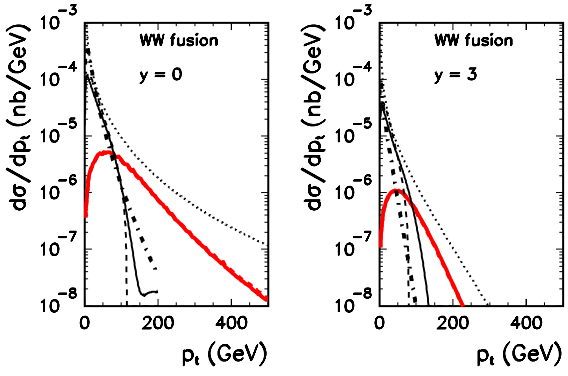

Fig. 18. Transverse momentum distribution of the Higgs boson at LHC energy, $W = 14\,\text{TeV}$ and $y = 0$ (left panel) and $y = \pm 3$ (right panel) produced in WW fusion (overlaping thick solid and thick dashed for the two different prescriptions specified in the formalism section), compared to the corresponding contribution of gluon–gluon fusion: the BFKL (dash-dotted), the Kwieciński (thin solid) UGDF, LO soft gluon resummation (dashed) and the perturbative $2 \to 2$ collinear contribution (thin dotted)

fusion. In particular, the maximum of the cross section at p_t slightly larger than 50 GeV is visible. It is interesting if the contribution of weak-boson fusion can exceed in some corner of the phase space the gluon–gluon contribution. In order to quantify the effect in Fig. 18 we present $\frac{d\sigma}{dy dp_t}$ as a function of the Higgs transverse momentum for $y = 0$ and $y = \pm 3$. The contribution of the WW fusion falls off much faster for $y = \pm 3$ than for $y = 0$. The results are almost independent of the choice of the factorization scale. These results almost coincide (compare thick solid (prescription (i) above) and overlaping thick dashed (prescription (ii) above) lines). For comparison we present a few examples of the gluon–gluon fusion with the BFKL (dash-dotted) and Kwieciński (thin solid) unintegrated gluon distributions and the standard resummation method with Gaussian form factor and $b_0 = 1\,\text{GeV}^{-1}$ (dashed). We find that depending slightly on UGDF and rapidity, above $p_t \sim 50$–$100\,\text{GeV}$ the WW fusion mechanism dominates over the gluon–gluon fusion mechanism. However, the $2 \to 2$ processes (dotted line) are large, especially at midrapidities. Only at large rapidities and $p_t > 150\,\text{GeV}$ the WW fusion seems to dominate over the other processes. However, there the cross section is rather small. Whether this opens a possibility to study the WWH and similarly the ZZH couplings requires further studies.

4 Conclusions

In the present paper we have presented predictions for the inclusive cross section for the Higgs boson production at the LHC energy $W = 14\,\text{TeV}$, obtained with the help of the different models of unintegrated gluon distributions used recently in the literature. Almost all the UGDFs discussed here were obtained based on the analysis of low-x HERA data for virtual photon–proton total cross sections. Although they are almost equivalent in the description of the HERA data, quite different results have been obtained for Higgs production. While the structure function data are sensitive to rather low transverse momenta of the gluon, in the Higgs production, in principle, one could sample the not yet explored region of large transverse momenta (at large scales). One should remember that the Higgs production even at large LHC energy is not completely a small-x phenomenon. The analysis of very forward or very backward Higgs boson production, in principle, could open a possibility to study UGDFs in a completely unexplored region of large x. This task, however, is by no means easy, as in this region of phase space "small-x" and "large-x" physics are entangled.

We have shown that for all UGDFs discussed here the inclusive cross section is dominated by the configurations with transverse momenta of the gluons smaller than the transverse momentum of the Higgs ($\kappa_1 < p_t$ and $\kappa_2 < p_t$).

Finally we wish to emphasize that the whole potential to study the UGDF in the Higgs production discussed here is at present only conditional as it implicitly assumes the existence, discovery and good identification of the Higgs boson in the future experiments at LHC. We do not need to mention that all this would not be possible if the Higgsless scenarios (see e.g. [35] and references therein) turned out to be true. Even if the Higgs boson is discovered at LHC the statistics may not be sufficient for precise tests of UGDF.

Acknowledgements. We are indebted to Krzysztof Golec-Biernat, Elżbieta Richter-Wąs and Tadeusz Szymocha for an interesting discussion and Krzysztof Kutak for providing us a routine for calculating the unintegrated gluon distributions from [26]. The paper has been improved thanks to suggestions of an anonymous referee. This work was partially supported by the grant of the Polish Ministry of Scientific Research and Information Technology number 1 P03B 028 28.

References

1. B. Anderson et al. (Small-x collaboration), Eur. Phys. J. C **25**, 77 (2002)
2. J. Andersen et al. (Small-x collaboration), Eur. Phys. J. C **35**, 67 (2004)

3. A. Szczurek, N.N. Nikolaev, W. Schäfer, J. Speth, Phys. Lett. B **500**, 254 (2001)
4. M. Łuszczak, A. Szczurek, Phys. Lett. B **59**, 291 (2004)
5. H. Jung, Mod. Phys. Lett. A **19**, 1 (2004)
6. A. Szczurek, Acta Phys. Polon. B **34**, 3191 (2003)
7. D. Kharzeev, E. Levin, Phys. Lett. B **523**, 79 (2001)
8. M.A. Kimber, A.D. Martin, M.G. Ryskin, Phys. Rev. D **63**, 114027 (2001)
9. J. Kwieciński, Acta Phys. Polon. B **33**, 1809 (2002)
10. A. Gawron, J. Kwieciński, Acta Phys. Polon. B **34**, 133 (2003)
11. A. Gawron, J. Kwieciński, W. Broniowski, Phys. Rev. D **68**, 054001 (2003)
12. J. Kwieciński, A. Szczurek, Nucl. Phys. B **680**, 164 (2004)
13. M. Czech, A. Szczurek, Phys. Rev. C **72**, 015202 (2005); nucl-th/0510007
14. R.K. Ellis, W.J. Stirling, B.R. Webber, QCD and collider physics (Cambridge University Press, Cambridge 1996)
15. M. Ciafaloni, Nucl. Phys. B **296**, 49 (1988); S. Catani, F. Fiorani, G. Marchesini, Phys. Lett. B **234**, 339 (1990); Nucl. Phys. B **336**, 18 (1990)
16. J.C. Collins, D. Soper, G. Sterman, Phys. Lett. B **109**(109), 388 (1982); Nucl. Phys. B **223**, 381 (1983); Phys. Lett. B **126**, 275 (1983); Nucl. Phys. B **250**, 199 (1985)
17. A. Gawron, J. Kwieciński, Phys. Rev. D **70**, 014003 (2004)
18. G. Watt, A.D. Martin, M.G. Ryskin, Phys. Rev. D **70**, 014012 (2004)
19. F. Hautmann, Phys. Lett. B **535**, 159 (2002)
20. A.V. Lipatov, N.P. Zotov, hep-ph/0501172
21. I. Hinchliffe, S.F. Novaes, Phys. Rev. D **38**, 3475 (1988); R.P. Kauffman, Phys. Rev. D **44**, 1415 (1991); C.-P. Yuan, Phys. Lett. B **283**, 395 (1992); C. Balazs, C.P. Yuan, Phys. Lett. B **478**, 192 (2000); C. Balazs, J. Huston, I. Puljak, Phys. Rev. D **63**, 014021 (2001); E.L. Berger, J.-W. Qiu, Phys. Rev. D **67**, 034026 (2003); G. Bozzi, S. Catani, D. de Florian, M. Grazzini, Phys. Lett. B **564**, 65 (2003)
22. A. Kulesza, W.J. Stirling, JHEP **0312**, 056 (2003)
23. A. Kulesza, G. Sterman, W. Vogelsang, hep-ph/0309264
24. K. Golec-Biernat, M. Wüsthoff, Phys. Rev. D **60**, 114023 (1999)
25. A.J. Askew, J. Kwieciński, A.D. Martin, P.J. Sutton, Phys. Rev. D **49**, 4402 (1994)
26. K. Kutak, A.M. Staśto, Eur. Phys. J. C **41**, 343 (2005)
27. J. Blümlein, talk at the workshop on Deep Inelastic Scattering and QCD, hep-ph/9506403
28. M. Glück, E. Reya, A. Vogt, Eur. Phys. J. C **5**, 461 (1998)
29. J.R. Ellis, M.K. Gaillard, D.V. Nanopoulos, Nucl. Phys. B **106**, 292 (1976)
30. V. Del Duca, W. Kilgore, C. Oleari, C. Schmidt, D. Zeppenfeld, Phys. Rev. D **67**, 073003 (2003)
31. R.K. Ellis, I. Hinchliffe, M. Soldate, J.J. van der Bij, Nucl. Phys. B **297**, 221 (1988); U. Baur, E.W.N. Glover, Nucl. Phys. B **339**, 38 (1990)
32. T. Figy, D. Zeppenfeld, C. Oleari, Phys. Rev. D **68**, 073005 (2003)
33. R.N. Cahn, S. Dawson, Phys. Lett. B **136**, 196 (1984)
34. ALEPH, DELPHI, L3, OPAL collaborations, LEP Electroweak Working Group and SLD Electroweak, Heavy Flavour Groups, hep-ex/0412015
35. R.S. Chivukula, H.-J. He, M. Kurachi, E.H. Simons, M. Tanabashi, Phys. Rev. D **70**, 075008 (2004); T. Nagasawa, M. Sakamoto, Prog. Theor. Phys. **112**, 629 (2004); Ch. Schwinn, Phys. Rev. D **69**, 116005 (2004); C. Csaki, C. Grojean, J. Hubisz, Y. Shirnan, J. Terning, Phys. Rev. D **70**, 015012 (2004)